ELSEVIER

Thermochimica Acta 267 (1995) 435–444

thermochimica acta

Very low-temperature heat capacities and magnetic thermal anomalies of the organic free radical magnet, 4-methacryloylamino-2,2,6,6-tetramethylpiperidine-1-oxyl (MATMP)[1]

Norihiro Ohmae[a], Atsushi Kajiwara[b], Yuji Miyazaki[a], Mikiharu Kamachi[b], Michio Sorai[a,*]

[a]*Microcalorimetry Research Center, Faculty of Science, Osaka University, Toyonaka, Osaka 560, Japan*
[b]*Department of Macromolecular Science, Faculty of Science, Osaka University, Toyonaka, Osaka 560, Japan*

Received 15 November 1995; accepted 4 May 1995

Abstract

The magnetic properties of 4-methacryloylamino-2,2,6,6-tetramethylpiperidine-1-oxyl (MATMP) have been investigated by means of adiabatic heat capacity calorimetry in the 0.08–24 K range. The heat capacities of MATMP showed a magnetic phase transition at 0.15 K and a hump centered around 1 K, arising from the short-range ordering characteristic of low-dimensional magnets. The entropy gain due to these two magnetic thermal anomalies was $\Delta S = 5.49$ J K^{-1} mol^{-1}. The hump can be well accounted for in terms of the spin $S = 1/2$ one-dimensional ferromagnetic Heisenberg model with an intrachain exchange interaction of $J_{\|}/k_B = 0.70$ K, where k_B is the Boltzmann constant. The temperature dependence of the magnetic heat capacities below the transition temperature is approximated by $T^{3/2}$. This fact, on the basis of the spin-wave theory, implies that MATMP would be a ferromagnet below the transition temperature. However, the magnetic susceptibility measurement reported recently suggests that MATMP would be antiferromagnetic below the transition temperature. A possible origin responsible for this contradictory feature is discussed.

Keywords: Very low temperature; Heat capacity; Magnetic thermal anomalies; 4-Methacryloylamino-2,2,6,6-tetramethylpiperidine-1-oxyl

* Corresponding author.

[1] Contribution No. 107 from the Microcalorimetry Research Center. Presented at the 30th Anniversary Conference of the Japan Society of Calorimetry and Thermal Analysis, Osaka, Japan, 31 October–2 November 1994.

SSDI 0040-6031 (95) 02501-4

1. Introduction

What are called "molecular-based magnets" have greatly attracted the attention of many researchers. They comprise organic molecular entities and exhibit spontaneous or sublattice magnetizations below critical temperatures. Their behavior contrasts with a classical image of diamagnetic organic molecules characterized by closed shell structures of electrons. Molecular-based magnetic materials have been designed and synthesized successively according to the idea offered by McConnel [1]. There have been reported three strategies to realize molecular-based magnets: charge transfer complexes, mixed metal complexes, and organic free radicals.

Most organic free radicals exhibit antiferromagnetic interactions between the adjacent radicals, but it has been reported that ferromagnetic interactions exist in several organic free radicals. Bis(2,2,6,6-tetramethyl-piperidine-4-yl-1-oxyl) suberate (TANOL suberate) has two-dimensional ferromagnetic coupling, although there is antiferromagnetic coupling between the planes, resulting in a metamagnet below 0.39 K [2,3]. The β-phase crystal of 2-(4′-nitrophenyl)-4,4,5,5-tetramethyl-4,5-dihydro-1*H*-imidazol-1-oxyl-3-*N*-oxide (*p*-NPNN) becomes a bulk ferromagnet below 0.6 K [4–8]. 1,3,5,7-Tetramethyl-2,6-diazaadamantane-*N*,*N*′-dioxyl is a ferromagnet below 1.48 K [9,10]. This is the highest transition temperature found so far for purely organic, non-ionic materials. New candidates for organic ferromagnets recently reported are the TEMPO derivatives (TEMPO, 2,2,6,6-tetramethylpiperidine-1-oxyl) [11,12], the α-phase crystal of HQNN (HQNN, 2-(2′,5′-dihydroxyphenyl)-4,4,5,5-tetramethyl-4,5-dihydro-1*H*-imidazolyl-1-oxy-3-oxide) [13], and so on.

The magnetic properties of 4-methacryloyloxy-2,2,6,6-tetramethylpiperidine-1-oxyl (MOTMP) and 4-acryloyloxy-2,2,6,6-tetramethylpiperidine-1-oxyl (AOTMP) shown in Fig. 1 have been investigated [14–19]. On the basis of the measurements of magnetic susceptibility, magnetization, and heat capacity, it has been indicated that MOTMP forms one-dimensional ferromagnetic chains with the intrachain interaction of $J/k_B = 0.45$ K and gives rise to a magnetic phase transition at 0.14 K, below which an antiferromagnetic

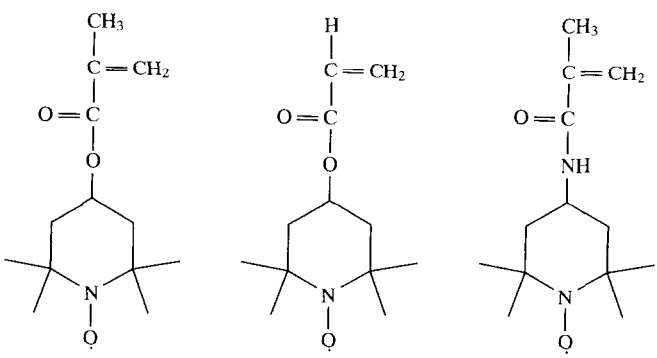

Fig. 1. Molecular structures of MOTMP, AOTMP and MATMP.

ordering is established with the interchain interactions of $J'/k_B = -0.02$ K and $J''/k_B = 0.035$ K. On the other hand, AOTMP is characterized by one-dimensional antiferromagnetic chains with $J/k_B = -1.25$ K and exhibits an antiferromagnetic phase transition at 0.64 K. Thus the intermolecular interaction of the radicals changes from antiferromagnetic to ferromagnetic by substituting the hydrogen atom at the α-position with a methyl group.

In the present study we treated 4-methacryloylamino-2,2,6,6-tetramethylpiperidine-1-oxyl (MATMP) shown in Fig. 1, which is an organic radical obtained by substituting the carboxyl group of MOTMP with an amido group. MATMP undergoes a magnetic phase transition at 0.16 K as detected by magnetic susceptibility measurements [19]. We describe the magnetic properties of MATMP on the basis of heat capacity measurements at very low temperatures.

2. Experimental

MATMP was synthesized according to the method given in the previous literature [20,21]. Heat capacity measurements were carried out in the temperature region from 0.08 to 24 K with a very low temperature adiabatic calorimeter workable with a ^{3}He/^{4}He dilution refrigerator [22]. Heat capacity measurements below 1 K were made under isoperibol conditions for 0.901 g (3.77×10^{-3} mol) of the sample forming a pellet of 20 mm in diameter and ~2 mm in thickness, while in the 1–24 K range an adiabatic calorimetry was made for a polycrystalline sample loaded in a gold-plated copper cell together with a small amount of ^{3}He gas as a heat exchanger. The mass of the specimen used for this measurement was 4.407 g (1.843×10^{-2} mol).

3. Results and discussion

Calorimetric results were evaluated in terms of the molar heat capacity at constant pressure C_p. The experimental data of MATMP are listed in Table 1. Fig. 2 shows the molar heat capacities of MATMP on a logarithmic scale. A sharp peak due to a magnetic phase transition was observed at 0.15 K. This is in good agreement with the transition temperature 0.16 K obtained from the magnetic susceptibility measurement [19]. Furthermore, we found a broad heat capacity anomaly centered around 1 K caused by the short-range ordering characteristic of low-dimensional magnets. This thermal behavior bears a close resemblance to that of MOTMP [14,15,18].

In order to separate the magnetic heat capacities from the observed values, we estimated the normal heat capacities by means of the following equation

$$C_p = a_1T^3 + a_2T^5 + a_3T^7 + a_4T^9 + a_5T^{-2} \quad (1)$$

The first four terms express the lattice heat capacities including the terms related to volume expansion such as T^5, T^7, and T^9. The last term originates in the short-range order of the spin system. A heat capacity anomaly arising from a short-range ordering is often

Table 1
Molar heat capacities of MATMP

T/K	C_p/J K^{-1} mol^{-1}	T/K	C_p/J K^{-1} mol^{-1}	T/K	C_p/J K^{-1} mol^{-1}	T/K	C_p/J K^{-1} mol^{-1}
Series 1		0.187	1.397	0.128	2.713	0.140	4.112
0.123	1.998	0.198	1.628	0.133	3.429	0.147	4.006
0.129	2.061	0.210	1.467	0.138	3.268	0.152	4.390
0.132	2.267	0.222	1.488	0.144	4.005	0.165	1.999
0.138	3.125	0.235	1.461	0.153	2.691	0.180	1.703
0.152	2.877	0.252	1.397	0.162	2.146		
0.171	1.842			0.175	1.819	Series 7	
0.190	1.937	Series 3		0.185	1.619	0.493	1.129
0.242	1.328	0.150	3.172	0.195	1.567	0.512	1.145
0.265	1.370	0.160	2.142	0.206	1.523	0.531	1.129
0.288	1.304	0.173	1.989	0.218	1.484	0.550	1.064
0.310	1.313	0.187	1.844	0.231	1.511	0.564	1.127
0.332	1.262	0.199	1.592	0.246	1.456	0.578	1.163
0.351	1.246	0.209	1.530			0.591	1.147
0.369	1.236	0.223	1.491	Series 5		0.602	1.136
0.386	1.235	0.238	1.441	0.075	1.126	0.614	1.066
0.401	1.244	0.254	1.398	0.082	1.196	0.623	1.130
0.410	1.208	0.269	1.357	0.088	1.453	0.634	1.149
0.429	1.185	0.284	1.365	0.093	1.416	0.644	1.125
0.450	1.176	0.301	1.332	0.098	1.909	0.655	1.129
0.468	1.182	0.323	1.286	0.105	1.806	0.669	1.079
0.487	1.156	0.346	1.255	0.113	2.009	0.691	1.094
0.504	1.172	0.367	1.225	0.119	2.608	0.718	1.094
0.519	1.191	0.388	1.236	0.126	2.382	0.744	1.080
0.534	1.182	0.408	1.216	0.133	2.918	0.767	1.090
0.541	1.098	0.426	1.199	0.140	3.566	0.787	1.026
0.549	1.167	0.441	1.191	0.146	3.417	0.802	1.068
0.561	1.156	0.455	1.186	0.153	3.142	0.819	1.011
		0.467	1.182	0.164	2.039	0.840	1.028
Series 2		0.477	1.206	0.178	1.971	0.860	1.033
0.111	2.100	0.486	1.164	0.189	1.431	0.876	1.056
0.116	1.765	0.504	1.133	0.198	1.559	0.891	1.069
0.119	2.074	0.527	1.119	0.212	1.487	0.903	1.033
0.123	2.388	0.555	1.131	0.227	1.464	0.915	0.993
0.127	2.885	0.594	1.102	0.241	1.376	0.929	0.962
0.132	3.272					0.942	0.977
0.137	3.399	Series 4		Series 6		0.963	0.983
0.141	3.582	0.088	1.384	0.076	1.052	0.988	0.941
0.145	5.695	0.093	1.720	0.086	1.481		
0.149	7.360	0.100	1.956	0.095	1.496	Series 8	
0.154	2.934	0.107	2.272	0.105	1.893	9.504	5.195
0.157	2.240	0.113	2.510	0.114	2.322	9.882	5.718
0.163	1.847	0.119	2.237	0.123	2.852	10.257	6.266
0.173	1.486	0.124	2.929	0.132	3.728	10.658	6.900

Table 1 (*continued*)

T/K	C_p/J K^{-1} mol^{-1}	T/K	C_p/J K^{-1} mol^{-1}	T/K	C_p/J K^{-1} mol^{-1}	T/K	C_p/J K^{-1} mol^{-1}
11.074	7.540	Series 9		2.241	0.429	8.073	3.388
11.507	8.249	1.109	0.837	2.453	0.409	8.545	3.951
11.956	9.040	1.229	0.765	2.687	0.380	9.039	4.563
12.423	9.855	1.384	0.700	2.918	0.379	9.558	5.251
12.884	10.848	1.601	0.611	3.181	0.384	10.106	6.025
13.340	11.485	1.843	0.520	4.859	0.766	10.684	6.935
14.304	13.263	2.099	0.507	5.242	0.941	11.298	7.908
14.812	14.255	2.355	0.412			11.892	8.823
15.335	15.366	2.642	0.384	Series 11		12.414	9.748
15.881	16.131	2.989	0.377	3.497	0.412	12.936	10.804
16.445	17.278	3.427	0.409	3.804	0.459	13.499	11.908
17.029	18.356	3.916	0.488	4.148	0.534	14.090	12.716
17.633	19.612	4.468	0.642	4.564	0.661	14.707	13.828
18.263	20.555			5.017	0.851	15.344	15.157
18.861	22.022	Series 10		5.514	1.098	16.015	16.253
19.388	22.891	1.312	0.749	5.973	1.381	16.715	17.512
19.993	24.314	1.490	0.659	6.388	1.687	17.390	18.966
20.719	25.618	1.681	0.584	6.799	2.017	18.005	20.030
22.233	28.638	1.853	0.530	7.200	2.371	18.698	21.655
23.037	30.391	2.042	0.474	7.623	2.829		
23.871	31.948						

found above a magnetic phase transition temperature and is known to be proportional to T^{-2} at high enough temperatures [23]. Hence the normal heat capacities are expressed by the first four terms of Eq. (1). The coefficients of Eq. (1) were determined to be $a_1 = 5.639 \times 10^{-3}$ J K^{-4} mol^{-1}, $a_2 = 3.134 \times 10^{-5}$ J K^{-6} mol^{-1}, $a_3 = -4.069 \times 10^{-7}$ J K^{-8}

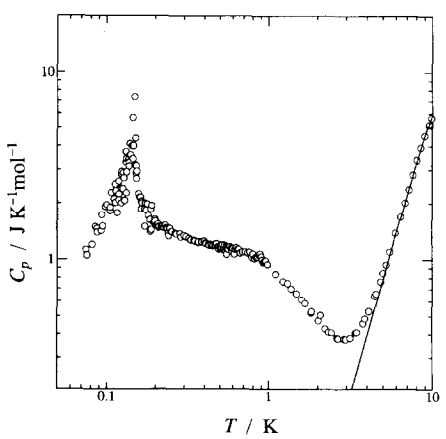

Fig. 2. Molar heat capacities of MATMP. Solid line indicates the normal heat capacity curve.

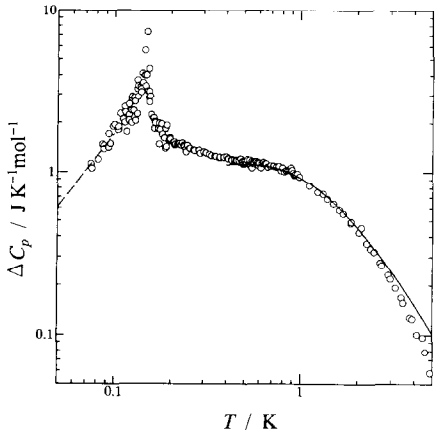

Fig. 3. Magnetic heat capacities of MATMP. Solid curve and broken line indicate the values by one-dimensional $S = 1/2$ ferromagnetic Heisenberg model and by the ferromagnetic spin-wave theory, Eq. (2) ($J_{\parallel}/k_B = 0.70$ K and $J_{\perp}/k_B = 0.02$ K), respectively.

mol^{-1}, $a_4 = 1.179 \times 10^{-9}$ J K^{-10} mol^{-1}, and $a_5 = 1.887$ J K mol^{-1} by fitting Eq. (1) to the experimental heat capacity data between 2 and 13 K. The derived normal heat capacity curve is drawn in Fig. 2 by a solid line.

The magnetic heat capacities ΔC_p obtained by subtracting the normal heat capacities from the whole heat capacities are plotted in Fig. 3 on a logarithmic scale. The magnetic entropy was evaluated by integrating the magnetic heat capacities with respect to ln T. The extrapolation of ΔC_p up to infinite temperature was performed by use of the T^{-2} term of Eq. (1), while that down to 0 K was done by use of the $T^{3/2}$ dependence of the magnetic heat capacities below 0.1 K. This temperature dependence derived from the spin-wave theory is mentioned below. The entropy gain thus determined was $\Delta S = 5.49$ J K^{-1} mol^{-1}, which agrees well with the theoretical entropy expected for a $S = 1/2$ spin system; $\Delta S = R \ln 2 = 5.76$ J K^{-1} mol^{-1}, where R is the gas constant. This fact indicates that the present specimen consists of pure MATMP radicals, each of which has a single unpaired electron, and that the observed heat capacity anomalies arise from the spin-spin interaction.

We first discuss the origin responsible for the hump of the magnetic heat capacities above the transition temperature. This anomaly is well fitted to the theoretical heat capacity curve estimated from the high temperature expansion of the $S = 1/2$ one-dimensional ferromagnetic Heisenberg model using Padé approximation [24]. This feature is shown in Fig. 3, in which a solid line corresponds to the theoretical curve. Based on this model, we estimated the intrachain exchange interaction to be $J_{\parallel}/k_B = 0.70$ K, where k_B is the Boltzmann constant. This value is slightly greater than the value for MOTMP ($J_{\parallel}/k_B = 0.45$–0.48 K) [15,16,18,19]. This ferromagnetic interaction is consistent with the Curie–Weiss behavior ($\theta \approx 0.7$ K) of the magnetic susceptibilities above the transition temperature [19].

In order to examine the nature of the phase transition at 0.15 K, we analyzed the heat capacities below the transition temperature in terms of spin-wave theory, which has proved to be a very valuable tool in describing the low-temperature properties of magnetic substances [25]. The heat capacity due to the spin-wave excitation in a three-dimensional ferromagnet possessing non-equivalent spin-spin interaction paths is given by the following equation [18]:

$$C_v = \frac{5R\zeta(5/2)\Gamma(5/2)}{16\pi^2 S^{3/2}}\left(\frac{k_B^3}{2J_1J_2J_3}\right)^{1/2} T^{3/2} \quad (J_1 > 0,\ J_2 > 0,\ J_3 > 0) \tag{2}$$

where J_1, J_2, and J_3 are the interaction parameters for three directions, ξ is Riemann's zeta function, Γ is Euler's gamma function, and S stands for the spin quantum number. On the other hand, the heat capacity arising from the spin wave in a magnet, where three ferromagnetic interaction parameters are fully or partially replaced by antiferromagnetic parameters, is expressed as follows [18]:

$$\begin{aligned} C_v &= \frac{R\zeta(4)\Gamma(4)k_B^3}{32\pi^2 S^3 V}T^3 \\ V &= \left(|J_1| + |J_2| + |J_3|\right)^{3/2}|J_1J_2J_3|^{1/2}/2 \quad (J_1 < 0,\ J_2 < 0,\ J_3 < 0) \\ V &= \left(|J_{21}| + |J_3|\right)^{3/2}|J_1J_2J_3|^{1/2}/2 \quad (J_1 > 0,\ J_2 < 0,\ J_3 < 0) \\ V &= J_1^2|J_2J_3|^{1/2}/2 \quad (J_1 < 0,\ J_2 > 0,\ J_3 > 0) \end{aligned} \tag{3}$$

From Eqs. (2) and (3) one can understand that the heat capacity of the spin wave in a three-dimensional ferromagnet is proportional to $T^{3/2}$, while in a three-dimensional antiferromagnet it is proportional to T^3. It should be remembered here that the temperature dependence of the spin-wave heat capacity drastically changes from $T^{3/2}$ to T^3 if only one of three ferromagnetic interactions is replaced by an antiferromagnetic nature. We fitted the following equation to the magnetic heat capacities below 0.1 K:

$$\Delta C_p = aT^{\alpha} \tag{4}$$

and obtained $\alpha = 1.57 \approx 3/2$. This suggests that the magnetic order of MATMP below the transition temperature would be of a ferromagnet. We thus adopt Eq. (2) for further discussion. As revealed by the short-range order effect seen above the transition temperature, the strongest magnetic interaction path in MATMP is the intrachain ferromagnetic interaction, whose intensity is determined to be $J_{\parallel}/k_B = 0.70$ K. The existence of weak interchain interactions brings about the magnetic phase transition at 0.15 K. At present we cannot discriminate two interaction parameters perpendicular to the magnetic chain. Therefore we assume $J_1 = J_{\parallel} = 0.70\ k_B$ K and $J_2 = J_3 = J_{\perp}$ in Eq. (2). Under this condition the best fit of Eq. (2) to the experimental ΔC_p data below 0.1 K was attained when $J_{\perp}/k_B = 0.02$ K. The theoretical curve thus determined is shown by a broken line in Fig.

3. The present result suggests that the ordered state below the transition temperature would be ferromagnetic because all three interaction parameters (J_1, J_2, and J_3) are positive.

However this conclusion derived from our calorimetric study seems to conflict with the magnetic measurement done for a single crystal of MATMP in the 0.035–1 K range by Takiguchi [19]. Prior to discussing reasons for the conflict between the two sets of experiments, a brief summary of his work is given here. (1) The temperature dependence of the AC magnetic susceptibility χ along three crystallographic axes demonstrates typical antiferromagnetic behavior, showing a magnetic order below ~0.16 K. (2) The magnetic field dependence of χ measured at 0.035 K exhibits a spin flop transition at the internal field of $H_{sf} = \sim 650$ Oe and the critical field is $H_{c\parallel} = \sim 1200$ Oe and $H_{c\perp} = \sim 1600$ Oe. Based on these values the average interchain interaction has been determined to be $J_\perp/k_B = -0.045$ K. (3) The magnetic susceptibilities at high temperatures are well approximated by one-dimensional the $S = 1/2$ ferromagnetic Heisenberg model with $J_\parallel/k_B = 0.70$ K, the same value as derived from our calorimetric study. However, when the phase transition temperature is approached, the model involving interchain interactions ($J_1/k_B = J_\parallel/k_B = 0.70$ K, $|J_2|/k_B + |J_3|/k_B = 0.042$ K) becomes a better approximation than the model without interchain interactions. He has assumed that both J_2 and J_3 might be negative, judging from negative $J_\perp$. (4) The magnetization measurements with a SQUID magnetometer under an extremely weak field of 0.01 Oe show a spontaneous magnetization along the crystallographic a-axis below 0.16 K, the phase transition temperature. Since the magnitude of the magnetization is extremely small (~1/4000) in comparison to normal ferromagnetic systems, he assumed a weak ferromagnetism arising from miscancellation of the magnetic moments of antiferromagnetically aligned spins.

As mentioned above, the spin-wave analysis is one of the most valuable tools in describing the low-temperature properties of magnetic substances, even in its most simple form, in which no account is taken of the interactions between the individually excited spin waves [25]. Therefore, unless the heat capacities in the 0.08–0.1 K range, to which the spin-wave theory was applied, unexpectedly involve large experimental error, the $T^{3/2}$ dependence cannot be discarded. Our calorimeter has been designed to be capable of measuring heat capacities down to 0.04 K [22]. In our experience the heat capacities in the 0.08–0.1 K range are usually determined without serious error. If this is the case, why does the present calorimetry lead to a ferromagnetically ordered state below the transition temperature in conflict with the magnetic study [19] suggesting an antiferromagnetic order? An explanation, although less probable, is that the temperature region (0.08–0.1 K), in which the spin-wave analysis was made, would be high for the spin-wave theory. At high temperatures the interactions between excited spin waves actually lead to a complicated temperature dependence of the spin-wave heat capacities. However, since the present temperature region corresponds to the region lower than two-thirds of the transition temperature, we think that this is a favorable region for the spin-wave theory in a normal sense.

An alternative account is that the weak ferromagnetism revealed by the magnetic measurement [19] would be reflected on the heat capacities as if MATMP was a bulk ferromagnet. Unfortunately we have no further idea, at present, to rationalize this possibility.

A final but not least interpretation is that the low dimensionality inherent in MATMP should be taken into account. The predicted limiting low-temperature behavior for systems of different dimensionality may be conveniently memorized by the formula $C_v \propto T^{d/n}$, where d is the dimensionality and n is defined as the exponent in the dispersion relation: for antiferromagnetic spin waves (magnons) $n = 1$ and for ferromagnetic magnons $n = 2$ [25]. Thus the spin-wave heat capacities of a three-dimensional ferromagnet go with $T^{3/2}$, those of a three-dimensional antiferromagnet go with T^3, and so on. Since there exist really no ideal low-dimensional systems, actual magnetic substances involve more or less high-dimensional components. The magnon which is first excited at low temperatures is the three-dimensional spin wave due to the weakest spin-spin interaction. As the spin-wave heat capacities arise from thermal excitation of magnons, we assumed $d = 3$ in the case of MATMP. Since the observed d/n ratio was 1.57, which is approximated as 3/2, we concluded $n = 2$, namely ferromagnetic ordering. On the contrary, if we a priori accept an antiferromagnetic order ($n = 1$), the dimensionality is reduced to $d = 1.57$. The fractional value of d might be a reflection of dimensional crossover.

The homologous compounds MOTMP and AOTMP are characterized as low-dimensional magnets and their spin-wave analysis gives $d/n = 1.53$ and 2.98 [14,18]. These values are well approximated by 3/2 and 3/1, respectively. Therefore the low dimensionality does not necessarily seem to bring about a small value for d. In the case of AOTMP both the inter- and intrachain interactions are antiferromagnetic [14,15,18]. Although MOTMP and MATMP are bulk antiferromagnets [16,19], they involve ferromagnetic chains [14,15,18,19]. For those complicated magnetic systems we formulated the spin-wave heat capacities as given by Eqs. (2) and (3). However, these equations correspond to only the first terms in high-temperature series expansions. Consequently the comparison between theory and experiment should be done at extremely low temperatures. In this regard the temperature regions used for the spin-wave analysis of MOTMP and MATMP would be too high.

The X-ray diffraction studies of the MOTMP, AOTMP, and MATMP crystals [15,17,19] revealed that they have similar crystal structures. In MOTMP and AOTMP crystals there are two superexchange interaction paths in the *ab*- and *ac*-planes, respectively. On the other hand, in the case of MATMP there is one superexchange interaction path along the *a*-axis. The difference of the magnetic properties between MOTMP and AOTMP may be caused by different orientation of the molecules: MOTMP molecules align parallel to the *b*-axis, while the orientation of AOTMP molecules is antiparallel to the *c*-axis. Therefore it is concluded that the magnetic properties of their radicals are determined by the intermolecular distances and the molecular orientations rather than by the molecular structures.

Acknowledgements

This work was supported by a Grant-in-Aid for Scientific Research on Priority Area "Molecular Magnetism" (Area No. 228/04242103 and 04242104) from the Ministry of Education, Science, and Culture, Japan.

References

[1] H. M. McConnel, J. Chem. Phys. (Paris), 39 (1963) 1910.
[2] G. Chouteau and Cl. Veyret-Jeandey, J. Phys., 42 (1981) 1441.
[3] A. Benoit, J. Flouquet, B. Gillon and J. Schweitzer, J. Magn. Magn. Mater, 31–34 (1983) 1155.
[4] M. Kinoshita, P. Turek, M. Tamura, K. Nozawa, D. Shiomi, Y. Nakazawa, M. Ishikawa, M. Takahashi, K. Awaga, T. Inabe and Y. Maruyama, Chem. Lett., 1225 (1991).
[5] M. Takahashi, P. Turek, Y. Nakazawa, M. Tamura, K. Nozawa, D. Shiomi, M. Ishikawa and M. Kinoshita, Phys. Rev. Lett., 67 (1991) 746.
[6] M. Tamura, Y. Nakazawa, D. Shiomi, K. Nozawa, Y. Hosokoshi, M. Ishikawa, M. Takahashi and M. Kinoshita, Chem. Phys. Lett., 186 (1991) 401.
[7] Y. Nakazawa, M. Tamura, N. Shirakawa, D. Shiomi, M. Takahashi, M. Kinoshita and M. Ishikawa, Phys. Rev. B, 46 (1992) 8906.
[8] M. Takahashi, M. Kinoshita and M. Ishikawa, J. Phys. Soc. Jpn., 61 (1992) 3745.
[9] R. Chiarelli, A. Rassat and P. Pey, J. Chem. Soc. Chem. Commun., 1081 (1992).
[10] R. Chiarelli, M.A. Novak, A. Rassat and J.L. Tholence, Nature, 363 (1993) 147.
[11] T. Nogami, K. Tomioka, T. Ishida, H. Yoshikawa, M. Yasui, F. Iwasaki, H. Iwamura, N. Takeda and M. Ishikawa, Chem. Lett., 29 (1994).
[12] T. Ishida, H. Tsuboi, T. Nogami, H. Yoshikawa, M. Yasui, F. Iwasaki, H. Iwamura, N. Takeda and M. Ishikawa, Chem. Lett., 919 (1994).
[13] T. Sugawara, M.M. Matsushita, A. Izuoka, N. Wada, N. Takeda and M. Ishikawa, J. Chem. Soc. Chem. Commun., 1723 (1994).
[14] H. Sugimoto, H. Aota, A. Harada, Y. Morishima, M. Kamachi, W. Mori, M. Kishita, N. Ohmae, M. Nakano and M. Sorai, Chem. Lett., 2095 (1991).
[15] M. Kamachi, H. Sugimoto, A. Kajiwara, A. Harada, Y. Morishima, W. Mori, N. Ohmae, M. Nakano, M. Sorai, T. Kobayashi and K. Amaya, Mol. Cryst. Liq. Cryst., 232 (1993) 53.
[16] T. Kobayashi, M. Takiguchi, K. Amaya, H. Sugimoto, A. Kajiwara, A. Harada and M. Kamachi, J. Phys. Soc. Jpn., 62 (1993) 3239.
[17] A. Kajiwara, H. Sugimoto and M. Kamachi, Bull. Chem. Soc. Jpn., 67 (1994) 2373.
[18] N. Ohmae, Master's Thesis, Osaka University, 1994.
[19] M. Takiguchi, Master's Thesis, Osaka University, 1994.
[20] T. Kurosaki, K.W. Lee and M. Okawara, J. Polym. Sci. Polym. Chem. Ed., 10 (1972) 3295.
[21] M. Kamachi, M. Tamaki, Y. Morishima, S. Nozakura, W. Mori and M. Kishita, Polymer J., 12 (1982) 362.
[22] S. Murakawa, T. Wakamatsu, M. Nakano, M. Sorai and H. Suga, J. Chem. Thermodyn., 19 (1987) 1275.
[23] M. Takahashi and M. Yamada, J. Phys. Soc. Jpn., 54 (1985) 2808.
[24] O.A. Baker, Jr., G.S. Rushbrook and H.E. Gilbert, Phys. Rev. A, 135 (1964) 1272.
[25] L.J. de Jongh and A.R. Miedema, Experiments on Simple Magnetic Model Systems, Sec. 4.2, Taylor & Francis, London, 1974.